Indian J Phys (October 2019) 93(10):1293–1299
https://doi.org/10.1007/s12648-019-01395-w

ORIGINAL PAPER

Negative-resistance behavior of bulk Ag_2O–TeO_2–V_2O_5 oxide glasses

D Souri[1]*, Z Esmaeili Tahan[2] and A Hakimyfard[2]

[1]Department of Physics, Faculty of Science, Malayer University, Malayer, Iran

[2]Department of Physics, Faculty of Science, Jundi-Shapur University of Technology, Dezful, Iran

Received: 30 June 2018 / Accepted: 29 November 2018 / Published online: 19 February 2019

Abstract: The bulk 3-component $x$$Ag_2O$–$40TeO_2$–$(60 - x)V_2O_5$ oxide glasses with different silver oxide contents of x = 0, 10, 20, 30, 40 and 50 mol% were prepared using the standard press-melt quenching method. The effect of the high DC electric field on the DC conductivity of the mentioned glasses was investigated using the gap-type electrode configuration. At the regime of low DC electric fields, the conduction of these samples was ohmic, whereas at high electric fields regime, present bulk samples show nonlinear behavior (i.e., non-ohmic conduction). The current–voltage characteristics show increasing deviation from Ohm's law with increasing current density, implying the non-ohmic behavior in close coincidence with Poole–Frenkel effect (PFE) which occurs at electrical fields nearly above 10^4 (V/cm); so, samples show the switching phenomena at a threshold voltage (V_{th}) from resistive state to conductive state. Based upon PFE, the lowering factor of potential barrier (β_{PF}) was determined for the understudied samples. Also, results show that generally the threshold voltage in which switching phenomenon occurs increases by increasing the electrode distance and decreases by increasing the sample temperature, but V_{th} shows two distinct regions of $0 \leq x \leq 20$ and $20 < x \leq 50$, in which the highest value of V_{th} is devoted to the case of x = 20 mol% with respect to other glasses; this result implies the structural change and then probable formation of crystallites in the amorphous matrix to be hard for the mentioned case, which is in good agreement with the previously reported mechanical aspects.

Keywords: Oxide glasses; High electric fields; Switching phenomenon; Poole–Frenkel effect (PFE)

PACS No.: 72.15.Cz

1. Introduction

Recently, tellurium oxide-based glasses have attracted a great interest due to their unique properties, such as high refractive index [1], high dielectric constants [2, 3] and high glass-forming ability [4, 5]. Also, these glasses have relatively high chemical stability, suitable mechanical strength [6, 7] and low melting point [8–10] beside their resistance against moisture for long times [9, 11], stability against devitrification and non-toxic feature [12]. Tellurium oxide (TeO_2) as a conditional glass former can readily form glass with a modifier such as an alkali metal oxide or alkaline earth metal oxide and also transition metal oxides (TMO_s) [13]. The basic structure of pure TeO_2 and tellurium oxide-based glasses consists of TeO_4 trigonal bipyramid (tbp). Also, glassy materials containing V_2O_5 have been proposed as cathode materials for lithium solid-state batteries [14–19]. Besides that, glasses containing noble metal oxides have been the subject of various investigations due to their potential as optical fiber lasers, amplifiers, scintillating glasses [20–22] and acousto-optical devices [23] and so forth. In some of the previous works, physical, electrical, optical and thermal properties of the different glasses like MoO_3–TeO_2–V_2O_5 [24], Sb_2O_3–TeO_2–V_2O_5 [25–27], Sb–TeO_2–V_2O_5 [9, 10, 28–32] and Ag_2O–TeO_2–V_2O_5 [33–36] have been studied. In the study of oxide glasses, one of the interested scientific fields is the high electric field phenomena and its mechanism, as will be discussed later. At electrical fields $\sim > 10^3$ V/cm, switching (high resistive state to high conduction state) or negative resistance phenomena were observed at a threshold voltage (V_{th}). Negative resistance characteristic means that under special conditions, the current will decrease with an increase in voltage [37]. Negative resistance and

*Corresponding author, E-mail: d.souri@gmail.com; d.souri@malayeru.ac.ir

electrical switching effects in materials can find applications in a variety of areas such as power control and information storage. The first reference to a switching in chalcogenide glasses occurred ~ 57 years ago (Ovshinsky, 1959), but a later paper by the same author (Ovshinsky, 1968) properly marked the in which its subject attracted of serious interests in solid-state electronics. The theoretical models and factors affecting switching and memory phenomena in chalcogenide glass are normally classified into "threshold" (or monostable) and "memory" (or bistable) devices. The threshold switching refers to the case in which continuous electrical power is required to maintain the highly conducting ON state; and memory switching refers to the case in which both ON and OFF states can be maintained without electrical power [38]. Different mechanisms have been proposed to explain the phenomenon of electrical switching in oxide and chalcogenide glasses. These include electronic, space charge, electrothermal and thermal mechanisms. It is now established more or less beyond doubt that in general, threshold switching is electronic in origin whereas memory switching is of thermal origin. Electrothermal mechanism becomes relevant while examining the influence of temperature on the various parameters that determine the switching behavior [39].

In the thermal mechanism, the transition from insulating to a conducting state is caused mainly by a joule heating effect, which is responsible for the increase in the temperature with the subsequent reversible phase transition. The electronic mechanism, developed for switching in thin films, assumes no heating of samples and results from space charges localized at the electrodes. The electrothermal mechanism, as a hybrid of two other mechanisms, is associated with the formation of both hot conductive channels in the material and space charges at electrodes [30]. The application of a high enough electric field causes Joule heating of the medium, which leads to crystallization of the glass into fine filaments. This results in excess carrier concentration in the current path [39]. In the family of oxide glass, vanadium-based glasses are usually found to exhibit electrical switching and high electrical conductivity. The investigation of the conductivity and switching behavior of these glasses can help to understand the mechanism of conduction and hence to select the suitable materials for device applications (e.g., memory switching and gas sensor). In our previous works, the optical [33], mechanical [34], some thermal properties [36] and also the low-field DC conductivity [35] of Ag_2O–TeO_2–V_2O_5 glasses have been studied. In the present work, the high-field conduction of the same glasses was investigated for the first time to complete their previously reported data. In our past work [35], for Ag_2O–TeO_2–V_2O_5 samples, the low-field DC electrical conductivity measurements were done within the temperature range of 150–380 K [34], and as mentioned before, the purpose of the present investigation is to study the high field electrical behavior of Ag_2O–TeO_2–V_2O_5 and extract some physical parameters such as threshold voltage and lowering factor of potential barrier, to more complete about the features of these glassy systems.

2. Experimental details

2.1. Preparation of bulk glasses and structural information

Glasses were prepared by the conventional melt quenching method. Bulk glass systems of $x$$Ag_2O$–$40TeO_2$–$(60 - x)V_2O_5$ with x = 0, 10, 20, 30, 40 and 50 mol% (hereafter termed as TVAgx) were prepared by mixing appropriate weights of raw TeO_2, V_2O_5 and Ag_2O materials; in this process, the precisely weighted and well-mixed starting raw powders were melted employing an electric furnace. It should be mentioned that during the melting process, regular stirring of the melt is mandatory to achieve the homogeneous melt; later, the melt was poured on to a steel block and pressed by another block. XRD patterns of TVAgx samples have been reported in our recent works [33–36], confirming their non-crystalline nature except for TVAg50. More details of the glass preparation process, structural characterization, glass density and some physical, thermal, optical and mechanical properties were described in our recent works [33–36].

2.2. Current–voltage (I–V) characteristics

Carefully, surface-polished bulk samples were used for electrical measurements, and electrical measurements were done with gap-type electrode configuration, using a high-voltage power supply (Molian Toos, 0–5 kV, Iran) and sensitive multimeters (TTi, 196, High-resolution computing multimeter, England). For each sample, the I–V characteristic was measured to verify the ohmic properties of the contacts. Also, the effect of different factors such as temperature and electrode distance on the I–V characteristic was investigated.

3. Results and discussion

3.1. Switching behavior and temperature dependence of threshold voltage ($V_{th}(T)$)

In this section, results of typical measurements on the I–V characteristics are shown in Fig. 1(a, b) for 2 different molar percentages of x = 10 and 20 mol% with a certain

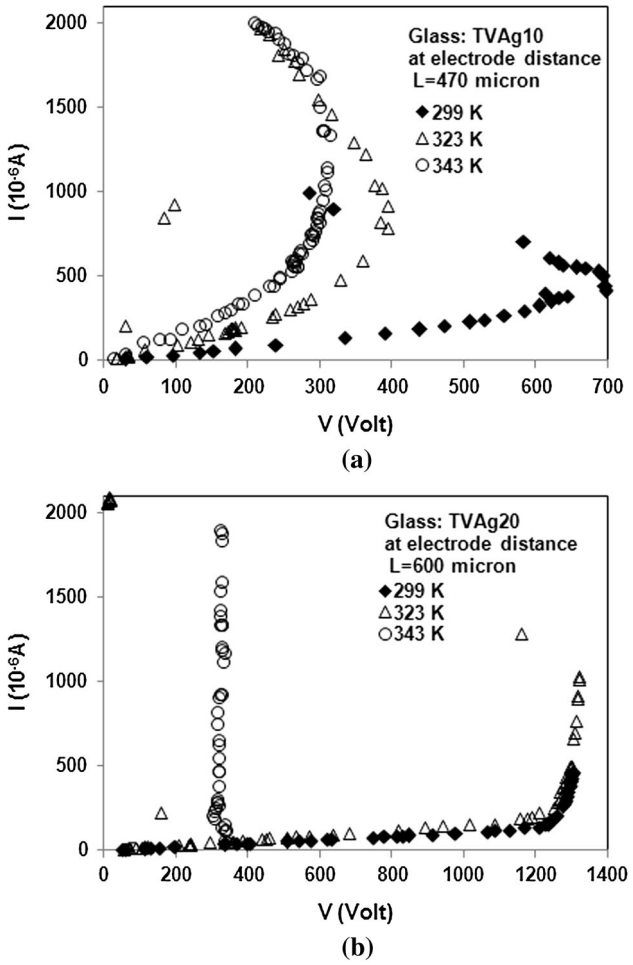

Fig. 1 (**a**) *I–V* characteristics of TVAg10 sample at 299, 323 and 343 K at a fixed electrode distance of 470 microns; (**b**) *I–V* characteristics of TVAg20 sample at different temperatures of 299, 323 and 343 K for a fixed electrode distance of 600 microns

electrode distance at different ambient temperatures. All obtained data of the mentioned samples and other studied samples are tabulated and summarized in Tables 1 and 2.

From Fig. 1(a, b),the increase in electrical conduction of glasses with increasing the temperature can be observed, which reveals the semiconducting nature of these samples. Also, during the experiments, the influence of Ag_2O content on the *I–V* characteristics was evident. The obtained results show the increase in resistivity with the increase in Ag_2O content up to $x = 20$ mol% and then decrease for the content of silver oxide above 20 mol%, showing the mixed polaronic-ionic origin of conduction (see Ref. [35]); this result is in agreement with the results of low-field DC conductivities reported in Ref. [35]. In other words, there is two region for V_{th}: $0 \leq x \leq 20$ and $20 < x \leq 50$, meaning a maximum at $x = 20$ mol% (i.e., substitution of V_2O_5 with Ag_2O and changing of the conduction mechanism from polaronic to mixed polaronic–ionic). As mentioned, it has been reported such behavior change in low DC electric

Table 1 Threshold voltage (V_{th}) at different electrode distances for TVAgx glasses (at room temperature of 299 K)

Glass name	Electrode distance (micron)	V_{th} (volt)
TVAg0	180	340.16
	380	524.46
	560	568.98
TVAg10	60	496.02
	120	586.92
	470	697.18
TVAg20	140	1249.05
	410	1262.65
	600	1279.33
TVAg30	230	1235.89
	320	1240.77
	530	1254.51
TVAg40	80	2.70
	120	433.09
	580	956.98
TVAg50	150	167.08
	250	206.69
	450	909.98

field experiments [35], which has been interpreted upon the change in the conduction mechanism at $x = 20$. Also, such behavior change has been reported in optical band gap [33], elastic velocities and moduli [34] and thermal stabilities [36], introducing $x = 20$ as a critical ratio of V_2O_5/Ag_2O; so, it is reasonable for a glass with higher thermal stability to have higher V_{th}, as discussed before. Besides that, it is evident from Fig. 1(a, b) that the samples exhibit an ohmic behavior in the high-resistance OFF state, and then deviate from ohmic behavior to reach the threshold voltage at which the sample shows a current-controlled negative resistance or switching behavior, which eventually leads to a low-resistance ON state. The samples are found to revert back to their high-resistance OFF state, when the current is reduced below the holding current, indicating a threshold-type electrical switching behavior. In other words, at low electric fields, the conduction of these samples was ohmic, while at high electric fields, bulk samples show nonlinear behavior (non-ohmic conduction). The current–voltage characteristics show increasing deviation from Ohm's law with increasing current density.

Actually, the results of studying the *I–V* curves show that the increase in temperature decreases the effect of the electric field to a certain extent. In other words, the electrical conductivity of the samples is influenced by both the temperature and the electric field.

Table 2 Data of threshold voltage (V_{th}), lowering factor of potential barrier (β_{PF}) and the square of correlation coefficient (R^2) at different temperatures, for TVAgx glasses

Glass name	Composition	Electrode distance (micron)	Temperature (K)	β_{PF} $(Vm)^{1/2}$	V_{th} (volt)	R^2
TVAg0	$40TeO_2$–$60V_2O_5$	380	299	6.89	340.16	0.998
			323	46.53	35.012	0.983
			343	55.15	28.938	0.949
TVAg10	$40TeO_2$–$50V_2O_5$–$10Ag_2O$	470	299	6.89	455.88	0.997
			323	12.06	288.41	0.990
			343	12.92	236.56	0.994
TVAg20	$40TeO_2$–$40V_2O_5$–$20Ag_2O$	600	299	4.31	1238.82	0.996
			323	5.17	1176.95	0.990
			343	9.48	335.44	1.00
TVAg30	$40TeO_2$–$30V_2O_5$–$30Ag_2O$	320	299	2.56	1202.67	0.995
			323	7.75	611.67	0.963
			343	9.48	362.02	0.935
TVAg40	$40TeO_2$–$20V_2O_5$–$40Ag_2O$	580	299	6.03	954.57	0.971
			323	27.57	26.226	0.863
			343	31.88	19.925	0.882
TVAg50	$40TeO_2$–$10V_2O_5$–$50Ag_2O$	450	299	6.03	909.98	0.996
			323	6.89	758.67	0.965
			343	0.06	205.526	0.981

Variation in threshold voltage of samples, with respect to temperature, is shown in Fig. 2. The threshold switching voltage data, obtained at different temperatures, are presented in Table 2. The results show that the threshold switching voltage of the glasses decreases with the increase in temperature as shown in Figs. 1(a, b) and 2, which is a common feature exhibited by other ternary glasses such as Sb–TeO_2–V_2O_5 [30], MoO_3–TeO_2–V_2O_5 [40–42], P_2O_5–Li_2MoO_4–Li_2O, P_2O_5–Na_2MoO_4–Na_2O [43] and CuO–ZnO–P_2O_5 [37].

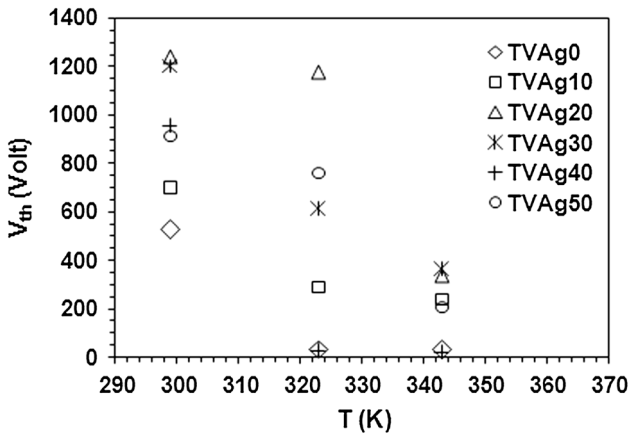

Fig. 2 Variation of threshold voltage with temperature, for TVAgx glasses

For the present TVAgx glasses, V_{th} has its highest value for TVAg20 with respect to other studied glasses; this result insists the structural change and then probable formation of crystallites in the amorphous matrix (along with the hot current filament) to be hard for TVAg20, which is in excellent agreement with the data of glass transition temperature and thermal stability of this glass composition, which can be followed from Ref. [36] and also from its mechanical and elastic moduli from Ref. [34].

3.2. Switching behavior and electrode distance dependence of threshold voltage (V_{th}(L))

The typical *I*–*V* characteristics of TVAg10 and TVAg20 systems for different electrode distances at the room temperature are shown in Fig. 3(a, b). For each sample, at a constant temperature, the increase in V_{th} with the increase in the electrode distance is evident. The increase in electrode distance increases the resistivity of the material between the electrodes and also increases the V_{th} (see Fig. 4 and Table 1, which report the complete data for all understudied samples). Also, it should be mentioned that (similar to what before-stated explanations for the case of different ambient temperatures) the highest value of V_{th} is devoted to TVAg20 with respect to other glasses; this result implies the structural change and then probable formation of crystallites in the amorphous matrix (along

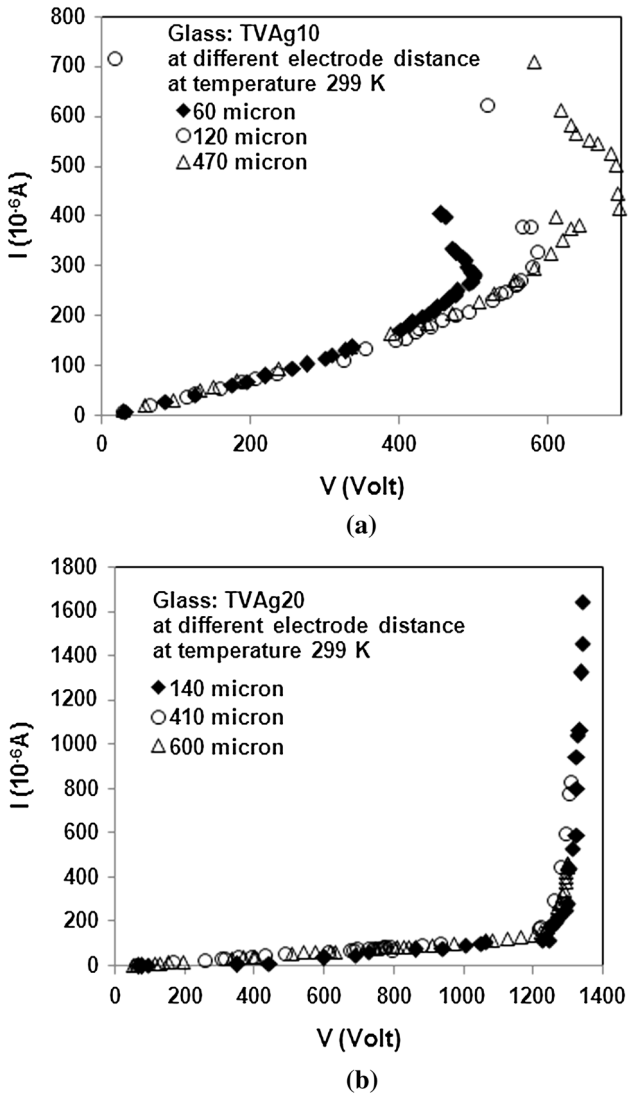

Fig. 3 (**a**) *I–V* characteristics of TVAg10 sample at different electrode distances at a fixed temperature. (**b**) *I–V* characteristics of TVAg20 sample at different electrode distances at a fixed temperature

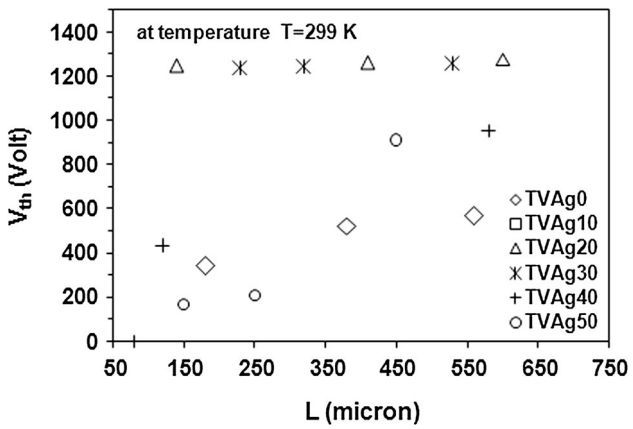

Fig. 4 Variation of threshold voltage with electrode distance, for TVAgx glasses

with the hot current filament) to be hard for TVAg20, which is in excellent agreement with the data of glass transition temperature and thermal stability of this glass composition, which can be followed from Ref. [36] and also from its mechanical and elastic moduli from Ref. [34].

3.3. Poole–Frenkel effect (PFE) and determination of lowering factor of the potential barrier

Curves of $T\ln(I)$ versus $E^{1/2}$ were plotted at different temperatures for different samples. Figure 5a shows the $T\ln(I) - E^{1/2}$ characteristics at different temperatures for TVAg20 sample. Also, Fig. 5b shows the fitting of the linear region of Fig. 5a at the temperature of 299 K. This review has been done at different temperatures for under-studied samples, but not shown in this article, and only the results of these studies are mentioned in Table 2. These figures show linear behavior at fields exceeding (10^3–10^4) V/cm as a bulk effect, based upon the Poole–Frenkel effect.

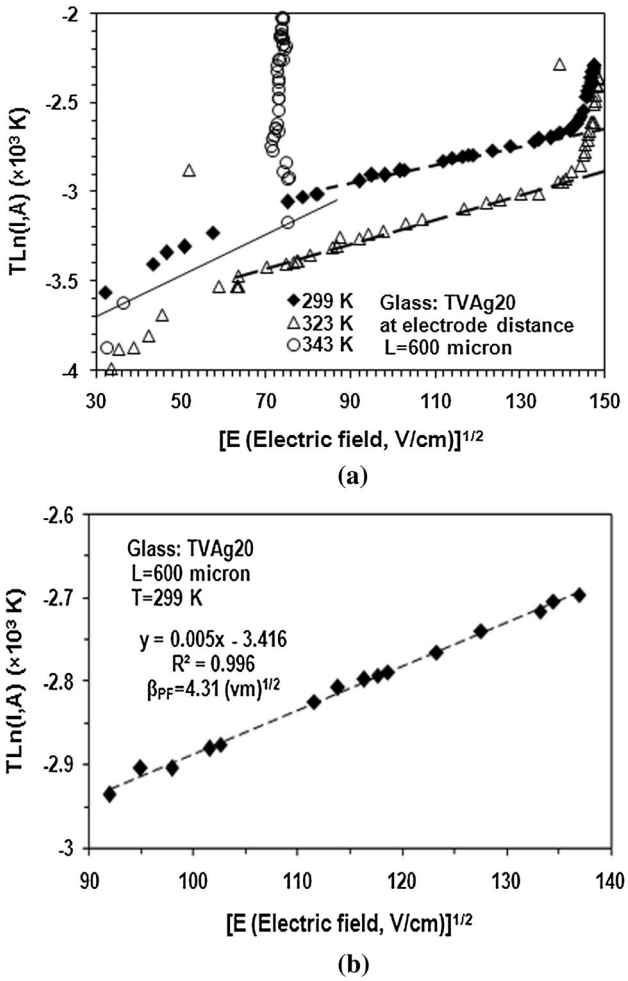

Fig. 5 (**a**) Plot of $T\ln(I)$ versus $E^{1/2}$ at different temperatures for TVAg20 glasses (dashed lines show the linear parts, which are drawn as a guide for the eye); (**b**) the fitting of the linear region shown in **a**

(E and I are the electric field and the electric current, respectively.)

The Poole–Frenkel effect is applicable if the trap center is neutral with the captured carrier (e^-, h^+), as only then an attractive (Coulomb) interaction is working when the charged carrier escapes from the charged trap. The general mechanism of the PFE is sketched in Fig. 6. The barrier $e_0\Phi_{tn} = |E_c - E_{tn}|$ for an electron to escape from its trap at energy level E_{tn} into the conduction band is equal in both directions in this simplified linear model for the field-free state ($E = 0$). This is changed by the presence of an electric field $E \neq 0$. In forward direction (in our case, the direction of the drift of the electrons), the barrier is diminished by $\Delta\phi_{PF}$ compared to the field-free state by the applied and/or internal electric field E with the appropriate sign. A field with the opposite sign enlarges the barrier in the same direction by about the same value. Usually, the Coulomb interaction between the leaving carrier and remaining charged trap is used [44].

We suppose that the material contains neutral impurity centers so that the potential energy of an electron or hole at distance x from these centers in the direction of electric field E is reduced relative to the state where the electric field is absent, namely:

$$\phi(x) = \frac{-e^2}{4\pi kx} - eE \cdot x \tag{1}$$

The maximum of the potential barrier occurs at $x_m = \frac{\beta_{PF}}{2E^{1/2}}$, where $\beta_{PF} = \left(\frac{e}{\pi k}\right)^{1/2}$ is the lowering factor.

Therefore, the probability of the thermal hopping P and current I *become* [41, 42, 45–47]:

$$p = \exp\left(\frac{-\phi_l}{KT}\right) \exp\left(\frac{e\,\beta_{PF}\,E^{1/2}}{KT}\right) \tag{2}$$

$$I \propto \exp\left(\frac{e\,\beta_{PF}\,E^{1/2}}{KT}\right) \tag{3}$$

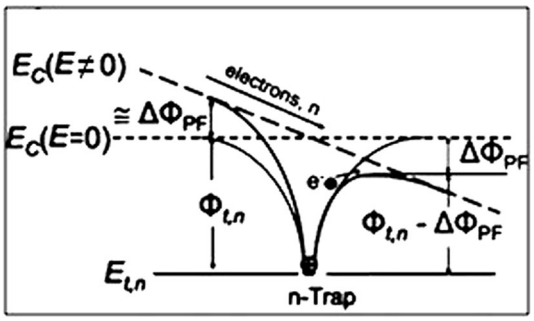

Fig. 6 Schematic sketch of the Poole–Frenkel effect without and with the electric field, E, [44]

$$\ln(I) = \text{Const} + \frac{e\,\beta_{PF}\,E^{1/2}}{KT} \tag{4}$$

An almost linear relation is obtained when the electric field is about 10^3–10^4 V/cm. As temperature increases for each sample, the field strength required for the onset of non-ohmic behavior is reduced due to increasing conduction with an increase in temperature (see Fig. 1a, b). Therefore, we can state that the Poole–Frenkel effect is thermal excitation caused by an electric field [46]. As the threshold voltage for the onset of negative resistance shows a decreasing trend with the increase in temperature and with the decrease in electrode distance (see Tables 1, 2), electrical behavior is interpreted by an electrothermal model. Details of the proposed model and further discussions are presented in Sect. 1.

Also, comparing the $I - V$ curves of each sample [Fig. 1(a, b)] at different temperatures, one can conclude that the present samples have a semiconducting nature (decreasing resistance with increasing temperature). Based on the results of the measurements presented in Fig. 5(a, b), one can determine the lowering factor β_{PF} of these glasses using the slope of the linear part of the $T\ln(I)$ versus $E^{1/2}$ curves. At different temperatures, for the understudied amorphous samples, we have employed the least-squares technique to determine the lowering factor β_{PF}. According to the above discussions, β_{PF} was determined for each sample (in SI units) and is listed in Table 2.

Results show that lowering factor of potential barrier of TVAgx samples in different temperatures increases with the increase in temperature for understudied samples except for TVAg50 at the temperature of 343 k. This behavior probably is due to the crystalline nature of TVAg50 sample, which is obtained from XRD [33]. From the regression analysis, the R^2 values were at the range of 0.863–1 for TVAgx (x = 0–50 mol%) (R is the correlation coefficient) as listed in Table 2. This analysis demonstrates a satisfactory fit to the data.

4. Conclusions

From the present work, the following aspects can be mentioned for xAg$_2$O–40TeO$_2$–(60 − x)V$_2$O$_5$ glasses:

1. The increase in electrical conduction of all glasses with increasing the temperature can be observed, which reveals the semiconducting nature of these samples. Also, the obtained results show the increasing resistivity with increasing Ag$_2$O content for $0 \leq x \leq 20$ mol%.
2. Threshold voltage depends on different parameters such as ambient (sample) temperature and electrode

distance. Results show that the threshold voltage at switching phenomenon increases and decreases with the increase in electrode distance and sample temperature for understudied samples, respectively.

3. As the threshold voltage for the onset of negative resistance shows a decreasing trend with the increase in temperature and with the decrease in electrode distance, electrical behavior is interpreted by an electrothermal model.
4. The highest value of V_{th} is devoted to the case of $x = 20$ mol% with respect to other glasses; this result implies the structural change and then probable formation of crystallites in the amorphous matrix (along with the hot current filament) to be hard for the mentioned case.
5. The electrical conductivity of the samples is influenced by both the temperature and the electric field.
6. The high electrical field experiments showed that at high field, *I–V* characteristic become non-ohmic as a result of lowering the potential barriers (Poole–Frenkel effect). Also, upon the Poole–Frenkel effect, lowering factor was determined for each sample (β_{PF}). For each sample, the β_{PF} value increases with the increase in temperature except for TVAg50 at the temperature of 343 k. This behavior probably is due to the crystalline nature of TVAg50 sample.

References

[1] D Souri *In book: Tellurite Glass Smart Materials, Springer*: ISBN: 978-3-319-76568-6, https://doi.org/10.1007/978-3-319-76568-6_5, 67–105 (2018)
[2] H M Moawad, H Jain, R El-Mallawany, T Ramadan and M El-Sharbiny *J. Am. Ceram. Soc.* **85** 2655 (2002)
[3] S E Ibrahim, Y S Rammah, I Z Hager and R El-Mallawany *J. Non-Cryst. Solids* **498** 443
[4] R El-Mallawany, *Tellurite Glass Smart Materials, Springer*: ISBN: 978-3-319-76568-6, https://doi.org/10.1007/978-3-319-76568-6_5, 1–17 (2018)
[5] I Z Hager and R El-Mallawany *J. Mater Sci.* **45** 897 (2010)
[6] I Z Hager, R El-Mallawany and A Bulou *Physica B* **406** 972 (2011)
[7] G Lakshminarayana, H Yang and J Qiu *J. Alloys. Compd.* **475** 569 (2009)
[8] M A Sidkey and M S Gaafar *Physica B* **348** 46 (2004)
[9] D Souri, H Zaliani, E Mirdawoodi and M Zendehzaban *Measurement* **82** 19 (2016)
[10] D Souri *Physica B: Condensed Matter* **456** 185 (2015)
[11] R El-Mallawany *Mater. Chem. Phys.* **53** 93 (1998)
[12] Y Gandhi, N K Mohan and N Veeraiah *J.Non-Cryst. Solids* **357** 1193 (2011)
[13] J C S Moraes, J A Nardi, S M Sidel, B G Mantovani, K Yukimitu, V C S Reynoso, L F Malmonge, N Ghofraniha, G Ruocco, L H C Andrade and S M Lima *J. Non-Cryst. Solids* **356** 2146 (2010)
[14] A Kaur, A Khanna, C Pesquera, F Gonzalez and V Sathe *J. Non-Cryst. Solids* **356** 864 (2010)
[15] Y B Saddeek, I S Syahia, W Dobrowolski, L Kilanski, N Romcevic and M Arciszewska *Optoelectron. Adv Mat.* **3** 559 (2009)
[16] I S Yahia, Y B Saddeek, G B Sakr, W Knoff, T Story, N Romcevic and W Dobrowolski, J. Magn. Magn. Mater. **321** 4039 (2009)
[17] V Rajendran, N Palanivelu, B K Chaudhuri and K Goswami *J. Non-Cryst. Solids* **320** 195 (2003)
[18] I Ardelean, C Marcus and R C Lucacel *Optoelectron. Adv Mat.* **9** 836 (2007)
[19] A G Kalampounias, G N Papatheodorou and S N Yannopoulos *J. Phys. Chem. Solids* **67** 725 (2006)
[20] S Gupta and A Mansingh *Philos. Mag. B* **78** (3) 265 (1998.
[21] M J Weber *J. Non-Cryst. Solids* **42** 189 (1980)
[22] M Oomen *Advanced Materials* **3** 403 (1991)
[23] A Abd El-Moneim *Mater. Chem. Phys.* **52** 36 (1998)
[24] D Souri *Measurement* **44** 1904 (2011)
[25] D Souri and Z Torkashvand *J. Electron. Mater.* **46 (4)** 2158 (2017)
[26] D Souri and Y Shahmoradi *J. Therm. Anal. Calorim.* **129 (1)** 601 (2017)
[27] D Souri *J.Mater. Sci.* **47 (2)** 625 (2012)
[28] D Souri *J. Non-Cryst. Solids* **470** 112 (2017)
[29] D Souri, Z Siahkali and M Moradi *J. Electron. Mater.* **45** (1) 307 (2016)
[30] D Souri, R Ghasemi and M Shiravand *J.Mater. Sci.* **50 (6)** 2554 (2015)
[31] D Souri, P Azizpour and H Zaliani *J. Electron. Mater.* **43 (9)** 3672 (2014)
[32] D Souri, M Mohammadi and H Zaliani *Electron. Mater. Lett.***10 (6)** 1103 (2014)
[33] D Souri and Z E Tahan *Appl. Phys. B: Lasers and Optics* **119** 273 (2015)
[34] D Souri, F Honarvar and Z E Tahan J. Alloys. Compd **699** 601 (2017)
[35] D Souri, Z E Tahan and S A Salehizadeh *Indian J. Phys.* **90** 407 (2016)
[36] D Souri *J. Non-Cryst. Solids* **475** (2017) 136
[37] M Mirzayi and M H Hekmatshoar *Physica B* **405** 4505 (2010)
[38] R A H El-Mallawany *Tellurite Glasses Hand book: physical properties and data, CRC Press, Second edition, ISBN: 9781439849835, Springer, 532 pages (2012)*
[39] R Rajesh and J Philip *Semicond. Sci. Technol.* **18** 133 (2003)
[40] H Hirashima, Y Watanabe and T Yoshida *J. Non-Cryst. Solids* **95**(96) 825 (1987)
[41] M Elahi and D Souri *Indian J. Pure. Appl. Phys.* **40** 620 (2002)
[42] D Souri and M Elahi *Czechoslovak. J Phys* **56**(4) 419 (2006)
[43] D Souri, M Elahi and M S Yazdanpanah *Cent. Eur. J. Phys.* **6**(2) 306 (2008)
[44] H Schroeder *J. Appl. Phys.* **117** 215103 (2015)
[45] M A Sidkey, R Elmallawany, R I Nakhla and A Abdelmoneim *J. Non-Cryst. Solids* 215 75 (1997)
[46] A K Jonscher, In: P.G. Lecomber, J. Mort (Eds.) *Electronic and structural properties of amorphous semiconductors* (Academic Press, London) p. 329 (1973)
[47] I G Austin and M Sayer *J. Phys. C* 7 905 (1974)